

Modeling wind ribs effects for numerical simulation external pressure load on a cooling tower of KAZERUN power plant-IRAN

Mohammad-Ali Goudarzi* and Saeed-Reza Sabbagh-Yazdi†

*Civil Engineering Department, K.N.Toosi University of Technology
No.1346 Valiasr Street, 19697- Tehran, Iran*

(Received July 29, 2008, Accepted October 20, 2008)

Abstract. In this paper, computer simulation of wind flow around a single cooling tower with louver support at the base in the KAZERUN power station in south part of IRAN is presented as a case study. ANSYS FLOTRAN, an unstructured finite element incompressible flow solver, is used for numerical investigation of wind induced pressure load on a single cooling tower. Since the effects of the wind ribs on external surface of the cooling tower shell which plays important role in formation of turbulent flow field, an innovative relation is introduced for modeling the effects of wind ribs on computation of wind pressure on cooling tower's shell. The introduced relation which follows the concept of equivalent sand roughness for the wall function is used in conjunction with two equations κ - ε turbulent model. In this work, the effects of variation in the height/spacing ratio of external wind ribs are numerically investigated. Conclusions are made by comparison between computed pressure loads on external surface of cooling tower and the VGB (German guideline for cooling tower design) suggestions.

Keywords: external surface wind ribs; natural draught cooling tower; finite element modeling; incompressible turbulent flow; wind pressure load.

1. Introduction

The geometrical features of the natural draught cooling towers of power plants make them vulnerable against storm. Wind ribs is placed on the cooling tower external surface and plays important role in formation of turbulent flow field and resulted pressure load (Fig. 1). This fact is considered in some of cooling tower design guidelines (like VGB [1]) for evaluation of wind induced pressure loads on cooling towers with standard shapes. However, modeling is recommended by most of the design guidelines for desired shape of the cooling tower considering ambient conditions.

A common modeling option is the use of laboratory models (i.e. placing small scale physical model in wind tunnel). This type of modeling only is time consuming and costly, but also it's results may encounter scaling errors when are applied to the full scale case. Positioning measuring devices and recording errors are some other problems associate with the laboratory models. The differences between the turbulent regime of flow in wind tunnel experiment and real world problem is one of

* PhD Candidate, Corresponding Author, E-mail: MAGoodarzi@alborz.kntu.ac.ir

† Associate Professor, E-mail: SYazdi@kntu.ac.ir



Fig. 1 General view of cooling towers wind ribs

the major source of scaling errors. The availability of high performance digital computers and development of efficient numerical models techniques have accelerated the use of Computational Fluid Dynamics. The control over properties and behavior of fluid flow and relative parameters are the advantages offered by CFD which make it suitable for the simulation of the applied problems.

There are various experimental efforts on small scale laboratory models (Tien & Liang 1980, Niemann, *et al.* 1980, 1998, Orlando 2001). A series of wind tunnel tests have been performed by Niemann, *et al.* (1980, 1998). In these experiments several issues such as distribution of wind pressure on external surface of cooling tower and interference effect of cooling tower and adjacent building have been investigated. Orlando (2001) also performed some experimental tests on a rigid model of two adjacent cooling towers. In this research Pressures measured on the two towers were compared with those registered on an isolated tower and interference factor for two cooling tower was suggested.

In the case of numerical works mainly the cross wind effect on the performance of NDCT are considered. Zhai and Fu (2002) developed the multi-block CFD algorithm and program to simulate the airflow and heat transfer in and around two cooling towers. Fu and Zhai (2001) had used their model to numerically investigate the effects of cross-wind on two in-line dry-cooling towers. They showed that the two-tower case exhibited different airflow and heat transfer patterns from the single tower. Zhai and Fu (2006) recently carried out an experimental and numerical research on the performance of wind-break walls underneath dry cooling towers that vertically placement at lateral sides of tower. Fisenko, *et al.* (2002) also developed a new approach to simulation performance of several types of cooling towers. Fisenko, *et al.* (2004, 2005) also applied this approach to a natural draft cooling tower with the pack to the performance simulation of mechanical draft cooling towers.

Unlike of performance simulation, numerical works are infrequently reported in literature to evaluate wind induced pressure field around NDCT. Liu, *et al.* (2006) proposed a CFD simulation method to obtain the wind load on large hyperbolic cooling tower. They showed the rationality of CFD method to obtain the wind load on cooling tower. Sabagh-Yazdi, *et al.* (2007) also developed a finite volume base model to evaluate the pressure and velocity field around NDCT. They used the model to study of the interference effect on three adjacent cooling towers and lateral building of KAZERON power plant located in south part of IRAN.

But in all mentioned researches the surfaces of cooling towers are assumed to be smooth and the effects of wind ribs on pressure field around NDCT in not considered. Geometrical modeling of wind

ribs is challenging due to the multiplicity and dimension smallness of wind ribs. Therefore relinquish of ribs effect leads to simplified numerical modeling of cooling towers. While, based on practical guide lines and pervious experimental investigations, the maximum wind pressure around a cooling tower could be reduced up to 60% by considering wind ribs on external surface of cooling towers.

Hence the main purpose of this study is to seek a remedy for numerical modeling of wind ribs.

Here, a three dimensional finite element incompressible turbulent flow-solver is utilized for computational modeling. An innovated relation is applied for modeling the effects of external ribs on formation turbulent flow field and wind induced pressure load. This method is developed using the concept of equivalent sand roughness in imposing wall function for calculating near wall velocity profile. The results of present modeling method are compared with pressure values suggested by VGB guide-line for a single cooling tower of KAZERUN power station (in south part of IRAN). In this work, the effects of various height/spacing ratios for wind ribs on formation of wind pressure load on the cooling tower shell are numerically investigated. The results of this numerical investigation are compared with the suggestions of VGB design code of practice. In order to provide better understanding about the flow field parameters, the computed results are presented in terms of color coded maps of pressure and velocity fields as well as velocity vectors on some sections and three dimensional figures of the cooling tower shell.

2. VGB guideline

According to VGB guidelines the external pressure is obtained from following relation:

$$W_e(Z, \theta) = C_p(\theta).q(z).\lambda \tag{1}$$

λ is a global amplification factor which depends upon the lowest natural frequency of the cooling tower ($1.0 < \lambda < 1.17$). It depends to the stiffness of the cooling tower shell (existence of stiffening rings as well as foundation and supporting condition). This amplification factor is considered as $\lambda = 1.0$ for KAZERUN power plant cooling towers. $C_p(\theta)$ is the external coefficient of pressure and represents the circumferential distribution of wind pressure load and is globally introduced as,

$$\begin{aligned}
 C_p(\theta) &= 1 - (2 + 0.1\alpha_k) \left[\sin \frac{90}{70 + \alpha_k} \theta \right]^{m_1} & 0 \leq \theta \leq 70 + \alpha_k \\
 C_p(\theta) &= 1 - (2 + 0.1\alpha_k) \left[\sin \frac{90}{70 + \alpha_k} \theta \right]^{m_1} & 0 \leq \theta \leq 70 + \alpha_k \\
 C_p(\theta) &= -1 + (0.5 + 0.1\alpha_k) \left\{ \sin \left[\frac{90}{20 + \alpha_k} (\theta - 70 - \alpha_k) \right] \right\}^{m_2} & 70 + \alpha_k \leq \theta \leq 90 + 2\alpha_k \\
 C_p(\theta) &= -0.5 & 90 + 2\alpha_k \leq \theta \leq 180
 \end{aligned} \tag{2}$$

For the side parts $m_2 = 2.395$ while m_1 and α_k as a function of surface roughness h/a (the height/spacing ratio of external wind ribs (Fig. 2), as tabulated in Table 1. The height/spacing ratios of the KAZERUN cooling towers wind ribs (with $h = 0.05$ m and $a = 1.96$ m), is considered as $h/a = 0.0255$.

Note that the surface roughness and external surface wind ribs have effects of on formation of turbulent flow field. In Fig. 3, the circumferential distributions of coefficient of pressure according to above relations are demonstrated for various surface roughnesses. $q(z)$ is the pressure due to the

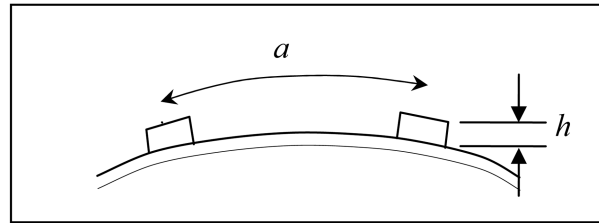


Fig. 2 Schematic features of the ribs

Table 1 The parameters for circumferential distribution of wind pressure coefficient

Surface Condition	h/a height/spacing ratio of external wind ribs	α_k	m_1
with wind ribs	0.025...0.100	0	2.267
	0.016...0.025	1	2.239
	0.010...0.016	2	2.205
	0.006...0.010	3	2.166
Without wind ribs	Off-shutter finish smooth	5	2.104
		6	2.085

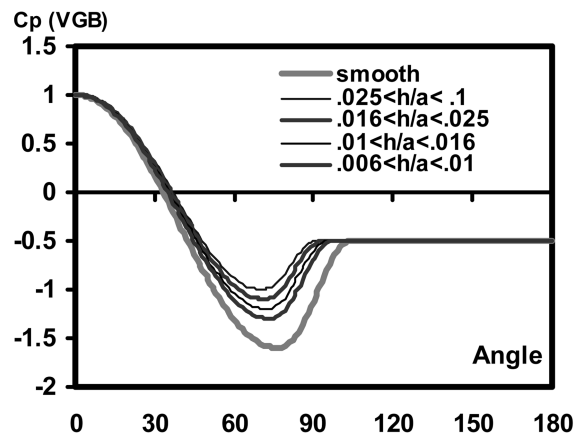


Fig. 3 Circumferential pressure distribution for various wind rib layouts

gust velocity and depends on the geographic location and the terrain category. The global profile of the pressure due to the gust velocity is defined as following relation:

$$q_z = \alpha_w \left(\frac{Z}{10} \right)^n \quad \text{KN/m}^2 \quad (3)$$

The power n is considered as 0.22 for interior parts of the Germany while it is considered as 0.17 in coastal zones. The values of α_w is calculated as a function of strongest 5 second gust wind. The gusty winds of various zones of the Germany are determined using W_{10} (the 60 minute gradient wind occurring with a return period of 50 years measured at 10 meter above ground level). The values of this coefficient depend on the geographic location and the terrain category. VGB recommends $0.71 < \alpha_w < 1.27$ for interior zones and $1.05 < \alpha_w < 1.52$ for coastal zones of the Germany. In present work, since KAZERUN power plant is located far from coastal zones,

$W_{10} = 41.2$ m/s, α_w and n are assumed as 1.06 and 0.22, respectively.

3. Computational model

In present investigations, the FLUTRAN module of ANSYS Finite Element Solver is utilized as a CFD tool. For CFD analysis, a three dimensional element (FLUID142), is used for all the numerical experiments of the work. This element type is designed for numerical solution of incompressible flow.

3.1. Incompressible flow equations

The utilized element (FLUID142) solves following set of equations which consist of continuity equation and equations of motion in i Cartesian direction, as ($j = 1,2,3$),

$$\frac{\partial u_j}{\partial x_j} = 0 \tag{4}$$

$$\frac{\partial u_j}{\partial t} + \frac{\partial u_i u_j}{\partial x_j} = -g_i - \frac{1}{\rho} \frac{\partial p}{\partial x_i} - \nu_e \left(\frac{\partial^2 u_i}{\partial x_j^2} \right) \tag{5}$$

Where $\nu_e = \nu + \nu_t$ is the equivalent eddy viscosity in which ν is fluid viscosity, while ν_t represent the turbulent flow viscosity of the flow. The turbulent flow viscosity appears in the equations of motion by considering analogy between Reynolds stresses (originated from adding the velocity fluctuations to the time average velocities, $u_i = u_i + u_i'$) and viscous stresses (Launder and Spalding 1974).

3.2. Turbulent model equations

In order to evaluate turbulent viscosity several models is introduced. Among various groups of turbulent viscosity models, successful results are reported in the literature for the two equation κ - ε models, particularly for three dimensional problems (Schlichting 1968). The standard κ - ε turbulent model introduces the turbulent flow viscosity as $\nu_t = C_\mu \kappa^2 / \varepsilon$, ($C_\mu = 0.09$). In this relation κ the kinematics energy of the turbulent and ε is its dissipation rate. In order to solve the flow equation considering the aforementioned relation for turbulent flow viscosity, it is necessary to define two equation for solving two extra unknowns κ and ε . The utilized element (FLUID142) solves following equations for solution of κ and ε ($j = 1,2,3$):

In which ϕ is the production term defined as:

$$\frac{\partial \kappa}{\partial t} + \frac{\partial u_j \kappa}{\partial x_j} = \frac{\partial}{\partial x_i} \left(\frac{\nu_t}{\sigma_\kappa} \frac{\partial \kappa}{\partial x_j} \right) + \nu_t \Phi - \varepsilon \tag{6}$$

$$\frac{\partial \varepsilon}{\partial t} + \frac{\partial u_j \varepsilon}{\partial x_j} = \frac{\partial}{\partial x_i} \left(\frac{\nu_t}{\sigma_\varepsilon} \frac{\partial \varepsilon}{\partial x_j} \right) + C_1 \nu_t \frac{\varepsilon}{\kappa} \Phi - C_2 \frac{\varepsilon^2}{\kappa} \tag{7}$$

$$\phi = \frac{\nu}{\rho} \left(\frac{\partial u_i}{\partial x_k} + \frac{\partial u_k}{\partial x_i} \right) \frac{\partial u_i}{\partial x_k} \quad (i = 1,2,3 \text{ and } k = 1,2,3) \tag{8}$$

For the standard κ - ε model certain constants are suggested as $C_1 = 1.44$, and $C_2 = 1.92$ (Schlichting1968).

3.3. Constant artificial viscosity

Artificial viscosity technique is employed to stabilize the solution procedure. Artificial viscosity enters the equations in the same manner as the fluid viscosity. This technique serves to increase the robustness of the finite element model in the regions with sharp gradients of flow parameters. Since the artificial viscosity is multiplied by the divergence of the velocity (zero for an incompressible fluid), it vanishes when the solution of incompressible flow converges to the steady state condition. According to user manual of the utilized software, the value of artificial viscosity should not exceed 1000 times the effective viscosity. In this work, the artificial viscosity value is set as 1 in initial stages of the computation.

4. Modeling wall roughness effect

4.1. Near wall velocity profile

Close to the wall boundary sharp velocity gradients form due to molecular viscosity of the fluid, and therefore, boundary layer develops. In this layer the effect of wall surface roughness on generation of viscous and turbulent stresses are pronounce. Because of high velocity gradient at fluid flow closed to the high resolution computational mesh is an essential requirement. However, this requirement may be relaxed by the use of algebraic formulation of velocity variations in the vicinity of the wall. In this concept the surface roughness plays an important role in the algebraic formulas of near wall velocity profile. In this work the effect of ribs (on the external surface of the cooling towers) is modeled using the analogy to surface roughness which is introduced as equivalent sand roughness in the standard formulations for near wall (White 1991).

For this propose, a brief description of general wall velocity profile law is reviewed here. For high Reynolds number flow over smooth walls, this law is formulated using dimensionless velocity and distance normal to wall surface as:

$$u^+ = \frac{u}{u_*}, \quad y^+ = \frac{u_* y}{\nu} \quad (9)$$

Using the velocity u tangent to the wall, fluid kinematics velocity ν , and friction velocity:

$$u_* = \sqrt{\tau_{wall}/\rho} \quad (\tau_{wall} : \text{near wall shear stress}) \quad (10)$$

For turbulent flow, the boundary layer is usually divided in to two major zones. The first zone namely sub-layer, closed to the wall surface ($y^+ < 11.6$), in which, the effects of kinematics viscosity of the fluid is dominated, the linear relation between velocity and wall shear stress ends up with $u^+ = y^+$. In the second zone ($30 < y^+ < 500$), in which, there is negligible variation in shear stress, logarithmic velocity profile forms can be described as follow:

$$u^+ = \frac{1}{k} \ln(y^+) + B \rightarrow u^+ = \frac{1}{k} \ln(Ey^+) \quad (\kappa = 0.42, E = 9.793) \quad (11)$$

The shear stress in the second zone is considered equal to wall shear stress. By equating the velocity for dimension velocity the criterion for laminar sub-layer thickness is obtained as:

$$\delta = \frac{11.6\nu}{u_*} \quad (12)$$

For rough walls the velocity profile in direction normal to the boundary is defined as [10]:

$$u^+ = \frac{1}{\kappa} \ln\left(\frac{y}{y_0}\right) \tag{13}$$

Where, y_0 is the actual surface roughness. Using K_s^+ which is known as Reynolds number roughness, describes the wall dimensionless roughness as:

$$K_s^+ = \frac{u^* K_s}{\nu} \tag{14}$$

Here K_s is the equivalent sand roughness. The values of $K_s^+ < 2.25$ represent smooth surface, while the values of $K_s^+ \geq 90$ are considered for roughness surface. The above relation is calibrated by laboratory measurements (Cebeci and Bradshaw 1977) as:

$$\frac{u}{u^*} = \frac{1}{\kappa} \ln\left(\frac{u^+}{K_s^+}\right) + 8.5 \tag{15}$$

Using above relation the dimensionless friction velocity u^* can be obtained for certain values of parallel wall velocity at normal distance y from the wall boundary with sand roughness K_s .

4.2. Modeling ribs roughness

Geometrical features of the surface wind ribs on external surface of the cooling tower, such as their height and spacing, play an important role on formation of turbulent flow parameters around cooling tower. The most important effect of ribs is reduction of the maximum negative pressure on both sides of cooling tower. Therefore, the effect of geometrical characteristic of ribs on the pressure load should be investigated properly which considered during the structural design and analysis. However, considering the actual geometrical features of the ribs for numerical analysis requires very fine mesh spacing, and hence, would ends up with heavy computational work load.

It should be noted that, accurate modeling of the wall surface roughness effects is an essential requirement for generation of viscous and turbulent stresses. This requirement is more pronounced in the boundary layer (close to the solid wall boundaries), where the sharp velocity gradients form. Therefore, high resolution computational mesh is required for computing the velocity gradient in the vicinity of solid wall boundaries. However, this requirement may be relaxed by the use of algebraic formulation for velocity profiles normal to the solid wall surfaces. In this concept, proper calculation of the surface roughness for the algebraic formulas plays an important role in obtaining realistic near wall velocity profile. The finite element analyzer software which is utilized in this work uses the relation (16) for near wall velocity profile.

$$u^+ = \frac{1}{\kappa} \ln \frac{y^+}{(1 + C_S K_s^+)} + 5.2 \quad (0 < C_S < 1) \tag{16}$$

The parameter K_s determines the roughness regime (smooth, transitional, or fully rough), where the value of zero implies a smooth wall (White 1991). C_S is an empirical dimensionless factor (between 0.5 and 1.0) that specifies the degree of non-uniformity of the surface roughness. The default value of 0.5 represents the uniform distribution of roughness K_s . Large values of C_S increase the

roughness effects without changing the flow regime defined by the value of K_s .

In this work, the effect of ribs is modeled using the analogy to surface roughness which is introduced as equivalent sand roughness in the standard formulations for near wall velocity profile.

For the rough surfaces ($K_s^+ > 90$), by assumption of ($1 + C_s K_s^+ \approx C_s K_s^+$), Eq. (16) could be expressed as:

$$\frac{u_p}{u^*} = \frac{1}{k} \ln \frac{u^* y_p}{\nu C_s K_s^+} + 5.2 \quad (17)$$

The relation between y_0 and K_s can be extracted by equating Eq. (17) and Eq. (13) as:

$$\frac{u_p}{u^*} = \frac{1}{k} \ln \frac{9.793 u^* y_p}{\nu C_s K_s^+} = \frac{1}{k} \ln \frac{y_p}{y_0} \Rightarrow K_s = \frac{E y_0}{C_s} \quad (E = 9.793) \quad (18)$$

This relation shows that effective modeling of the turbulent flow over rough surfaces the equivalent sand roughness K_s should be considerably larger than the actual surface roughness y_0 .

Extending this concept, we can reason that the geometrical parameter h/a describes the intensity of the roughness of external surface of the cooling tower. In order to develop a realistic relation between the geometrical parameter of the ribs (h/a) and the concept of equivalent sand roughness, following relation is introduced in present work:

$$K_s = C \left(\frac{h}{a} \right) h \quad (19)$$

Here, the coefficient C can be considered as $C = 20E/C_s$ ($E=9.793$). Thus, the height-spacing ratio (h/a) is used as a dimensionless number which properly weights the roughness effect. The above equation should be calibrated with measured data. Due to the fact that the maximum negative pressure in both side of a cooling tower is only sensitive to the surface roughness, the result of the introduced modeling strategy will compared will experimental and field measurements over a different range of height-spacing ratio of ribs for the case of full scale modeling. In the case of small scale experimental modeling of wind ribs, the reliable data is very rare. However the result of numerical modeling of small scale cooling tower, using proposed strategy, is compared with the result of reported data in literature (Orlando 2001) in next section.

5. Boundary conditions

5.1. Wall boundary condition

By application of above mentioned technique, no-slip condition is imposed on solid wall boundaries by setting the wind velocity components on the ground and cooling tower surfaces to zero value. The pseudo surface at top of the cooling tower is considered as free slip impermeable boundaries. The side and top far field boundaries are considered as symmetry (free slip) boundaries.

5.2. Flow boundary condition

Applying the proper boundary condition is one of the important points of numerical modeling. A brief description of boundary condition applied in current work is presented in this section.

For the modeling of the wind flow around a cooling tower, the inflow and outflow boundary are considered at distances 3.5 times of cooling tower diameter far from the object. Since the wind flow

usually produces turbulent velocity profile near ground surface, similar velocity profile is imposed at inflow boundary and atmospheric pressure is considered as the outflow boundary condition. However, for the top and side boundaries of computational domain symmetry boundary condition is applied by considering zero normal velocity. The atmospheric pressure ($p = 0$) is considered at outflow boundary and velocity profile is imposed at inflow boundary.

6. Modeling verification on small scale tower

In order to evaluate the accuracy of the results of two modeling strategy on formation of turbulent wind induced force on external surface on the NDCT(Natural Draft Cooling Tower), a set of pressure measurements on a small scale laboratory model (1/300 scale of the prototype) are used (Fig. 4 and Table 2)(Orlando 2001). For this purpose, the dimensions of the physical model are used for digital geometrical modeling of computational field.

In the physical model, the spacing between V shape columns (legs) at the tower footing were simulated by considering 36 circular holes at the footing (Fig. 5). However, these holes are not considered in the numerical model, and in turn, the footing part of the NDCT is considered as a fully permeable (part of the flow domain). Thus, a free slip horizontal disk is imposed not only on the top of NDCT, but also at the footing of the tower shell, above the elevation of V legs.

The 24 SWR with 0.4 mm height on the NDCT surface of the small scale model are not geometrically modeled in the numerical mesh. In turn, their effects on the solution are considered by application of the concept of equivalent sand grain roughness introduced in this work. Therefore,

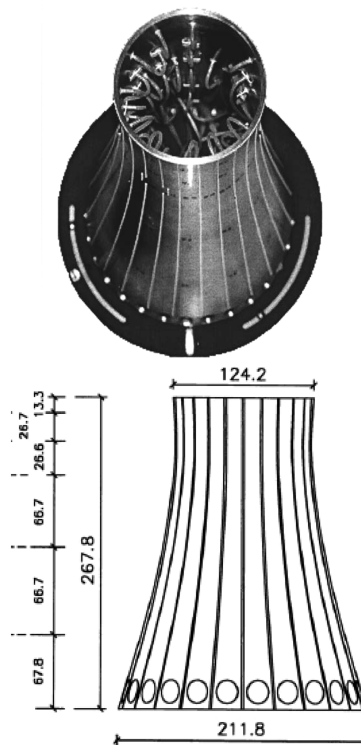


Fig. 4 Small scale experimental cooling tower geometry

Table 2 Geometrical specifications of small scale NDCT [6]

Level ID	Radius (mm)	Height (mm)
Base	105.9	0
Lower shell edge	103.4	30.5
Throat level	60.2	227.8
Upper shell edge	62.1	267.8

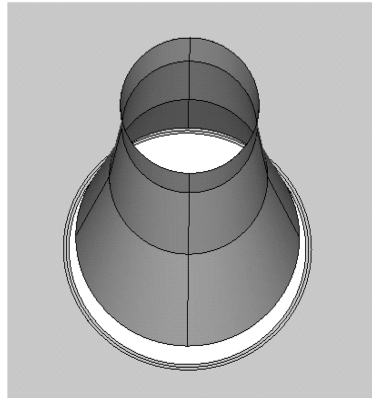


Fig. 5 Computational geometry model

corresponding to the geometrical features of SWR on physical model surface, the height/spacing ratio (h/a) as $3 \cdot 10^{-2}$ and $h=0.4$ mm are applied for computation of equivalent sand roughness.

In order to provide proper conditions for formation of velocity gradients, some circular structured layers of finite elements are considered in the vicinity of NDCT shell. In these layers, the elements are increased regularly around the NDCT wall, and then, far from the NDCT, unstructured mesh is developed.

As the flow boundary conditions, atmospheric pressure at down stream flow boundary and following relation for velocity profile at inflow boundary are imposed.

$$u^+ = \frac{u_*}{\kappa} \ln\left(\frac{z}{z_0}\right) \quad (u_* = 1.809 \text{ m/s}, z_0 = 3.431 \text{ mm}) \quad (20)$$

The computations of this test are performed in two stages. At first, the steady state solution is achieved by neglecting the ribs effects considering smooth condition for tower surface ($K_s = 0$). Then, in the second stage the rough condition is imposed by considering SWR effects in the next stage of computation. For both stages, the root mean square of the pressure is considered as a criterion for checking the convergence toward steady state. The computational procedure of both stages is stopped when the pressure root mean square reduced by the order of 6.

Fig. 6 presents the color coded maps of computed pressure field. Fig. 7. presents the comparison between the measured pressure coefficients at throat level of NDCT with computed results (for two conditions of smooth and rough external surface of NDCT). The effect of surface roughness modeling on reduction of the negative pressure at NDCT sides is clearly appeared in this figure. From the values tabulated in Table 3, it can be concluded that the computed external pressures at throat level are in close agreements with experimental measurements, particularly if the surface roughness is modeled by introduced concept of equivalent sand roughness.

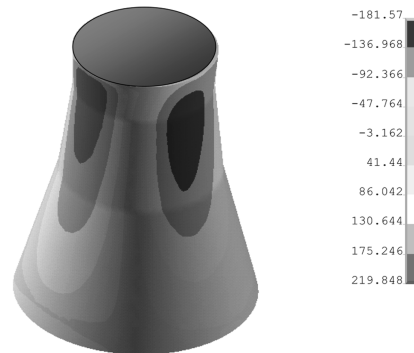


Fig. 6 Color coded map of computed pressure values on experimental cooling tower external surface

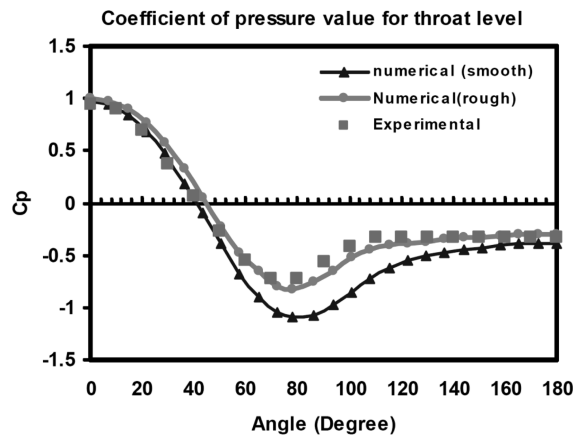


Fig. 7 Circumferential distribution of computed coefficient of pressure at throat level of a small scale NDCT

Table 3 Error on computed C_p in throat level for small scale NDCT

θ°	Exp.	Num Rough	Num. smooth	ERROR with Exp (rough)	ERROR with Exp (smooth)
0	0.95	1	.97	5	2.06
30	0.37	0.57	0.48	35	22.9
60	-0.55	-0.48	-0.67	14.5	17.9
90	-0.56	-0.64	-0.97	12.5	42.2
120	-0.33	-0.38	-0.55	13.15	40
150	-0.33	-0.32	-0.42	3.12	21.42
180	-0.33	-0.3	-0.38	10	13.15
			Mean:	13.35%	22%

7. Case study for pressure load modeling

In this section, the accuracy of the introduced technique for modeling the effects of ribs on external surface of a full scale cooling tower is investigated. For this purpose, one of the cooling towers of KAZERUN power plant (Iran) is chosen and its geometric feature (including the base structure and external wind ribs) are model with actual dimensions (Fig. 8). Considering single

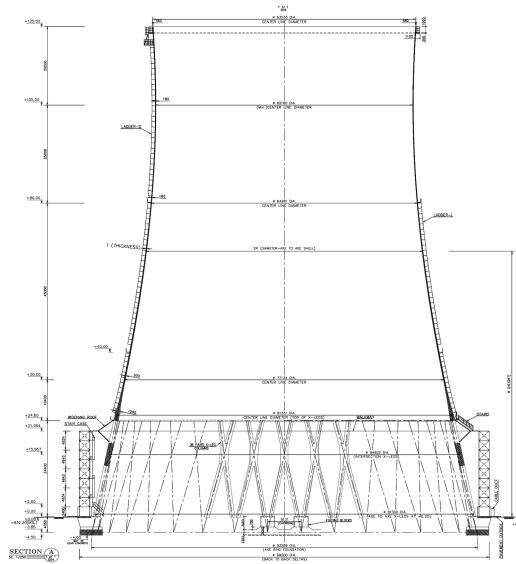


Fig. 8 Full scale cooling tower geometry with supporting structures for the louvers at its base (KAZERUN power plant - IRAN)

cooling tower and neglecting the interference effects is based on VGB guide line state about group of cooling towers. In this case VGB codes declares that if the distance of central point of two neighbor cooling towers is more than 3 times of average diameter of towers, the interference effect could be negligible. This expression is supported by a large number of experimental works Orlando (2001). In the case of KAZ ERUN power plant towers the interference effect has been investigated by the authors (Sabagh-Yazdi, *et al.* 2007). The results show no interference effects between cooling towers for the main direction of wind flow. Therefore only one cooling tower is considered here.

7.1. Computer modeling results

Unstructured mesh of tetrahedral is used for converting the flow domain into discrete form. This mesh is generated by generating 912054 elements (Fig. 9).

It should be noted that, since the pervious works in the literature report blockage flow conditions at top of the cooling towers for high speed wind flow, in this work the trapped flow inside the cooling tower is neglected for the seek of computational efficiency. The blockage condition is numerically model by considering one free slip disk at the top of the computational model (Fig. 10). Applying free slip disk, the wind flow is not allowed to circulate inside the cooling tower. Therefore the inside part of cooling tower is not considered in numerical model and the vertical component of fluid velocity is considered to be zero on the roof of the tank.

The atmospheric pressure ($p = 0$) is considered at outflow boundary and flowing velocity profile is imposed at in flow boundary:

$$V_z = 41.2 \left(\frac{Z}{10} \right)^{0.11} \quad (21)$$

Flow-induced forces on curved bodies, like cooling towers, depend strongly upon Reynolds number (R_e). Considering above equation, the wind velocity is more than 41.2 m/s in main part of undisturbed

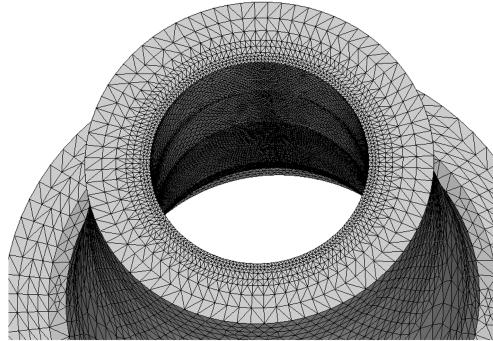


Fig. 9 Arranging structured finite elements mesh around the cooling tower shell

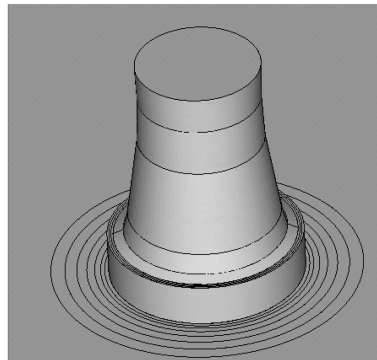


Fig. 10 Free slip disk at the top of the computational model

flow domain. Therefore the Reynolds number for considered cooling tower could be obtained by:

$$R_e = \left(\frac{1}{\mu}\right)\rho V D = \left(\frac{10^5}{1.8} \text{m.s/Kg}\right)(1.205 \text{Kg/m}^3 * 41.2 \text{m/s} * 90 \text{m}) = 24 * 10^7 \quad (22)$$

Where V is the mean velocity of the undisturbed flow, D is the mean tower diameter and ν is the kinematic viscosity of air. The Reynolds number is large enough to consider the turbulent flow around the cooling tower.

The proposed technique for equivalent surface roughness effect of wind ribs for actual height/spacing ratios (h/a), of the KAZERUN cooling towers (with $h = 0.05$ m and $a = 1.96$ m) is applied. Hence, the equivalent sand roughness is considered as $K_s = 0.0255$.

The numerical computations start with the case of smooth cooling tower surface ($h/a=0$) until the solution converges after 2500 iterations by reduction of 6 orders of magnitude in pressure root mean squares. Then, by application of the introduced relation for equivalent sand roughness, the rough condition is imposed for the cooling tower shell for this case the solution was converges after 1500 iterations and reduction of pressure root mean square up to value less than $2.5 * 10^5$.

In following figures (Fig. 11, 12, 13 and 14) the color coded maps of the velocity and pressure field around cooling tower are presented.

7.2. Comparing with VGB guideline

In order to verify the results of proposed technique for equivalent surface roughness effect of wind

ribs for various height/spacing ratios (h/a), an applied range of this ratio ($0 < h/a < 0.1$) is examined in present numerical investigation. In this work, seven value of h/a (with constant $h = 0.05$) are considered. The calculated equivalent sand roughness, K_s , of the cases is tabulated in Table 4.

The numerical computations start with the case of smooth cooling tower surface ($h/a=0$) until the solution converges after 2500 iterations by reduction of 5 orders of magnitude in pressure root mean squares. Thereafter, the six nonzero equivalent sand roughness cases are examined by starting from

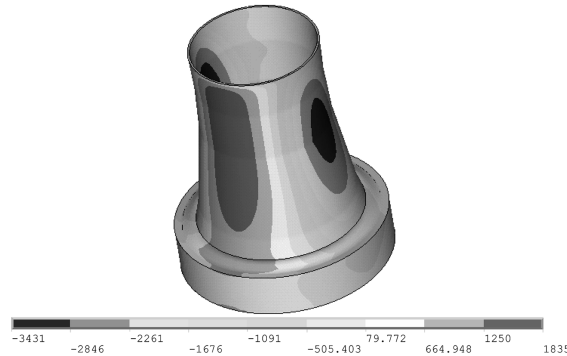


Fig. 11 Color coded map of pressure on upstream surface of the KAZERUN cooling tower ($h/a = 0$) (N/m^2)

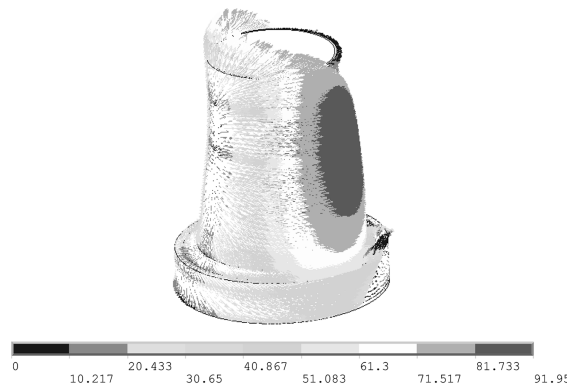


Fig. 12 Color coded velocity vectors on upstream surface of the KAZERUN cooling tower (m/s)

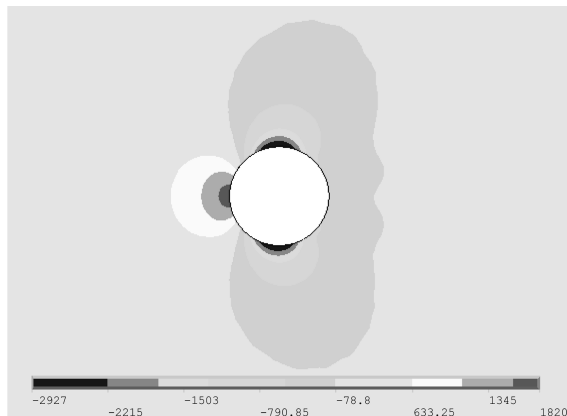


Fig. 13 Color coded map of pressure field on a horizontal surface passing through throat of the KAZERUN cooling tower (N/m^2)

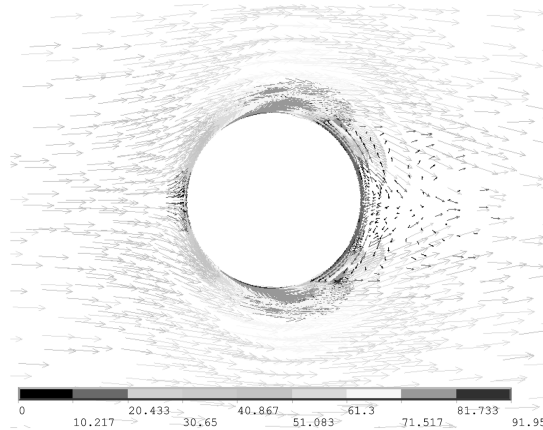


Fig. 14 Color coded map of velocity vector on a horizontal surface passing through throat of the KAZERUN cooling tower (m/s)

Table 4 Dimension of ribs and related equivalent sand grain roughness

ID	h/a	Equivalent sand grain Roughness (K_s)
No.1	0.1	0.97
No.2	0.05	0.485
No.3	0.025	0.2425
No.4	0.016	0.1552
No.5	0.01	0.097
No.6	0.006	0.0582
No.7	smooth	0

the solution for smooth surface ($h/a = 0$). For each cases the solution was converges after 1500 iterations and reduction of pressure root mean square up to value less than $2.5 * 10^5$. Comparison of the circumferential pressure coefficient diagram for the seven cases present similar trends at throat level (Fig. 15). Identical positive coefficient of pressure ($C_p = 1$) were computed at upstream stagnation point ($\theta = 0$) for all the height/spacing ratios. The maximum negative coefficient of pressure on both cooling tower sides varies ($-0.85 < cp < -1.5$), while their position moves toward upstream ($70 < \theta < 90$) and ($278 < \theta < 290$) for various height/spacing ratios ($0 < h/a < 0.1$). A constant value of negative pressure are computed at downstream part of the cooling tower ($120 < \theta < 240$) shell for all the six cases with surface roughness. However, for the case with smooth surface, similar constant negative pressure is computed in relatively smaller zone ($140 < \theta < 220$). The comparison is made between the experimental measurement and numerical results using the dimensionless pressure coefficient as:

$$C_{pi} = \frac{2(p_0 - p_i)}{\rho U^2} \tag{23}$$

Here, p_i is the pressure at desired computational node, where p_0 is the free stream pressure at out flow and U is the free-stream velocity (at the same level of node i) imposed at inflow boundary. Fig. 15 shows that, the maximum computed negative pressures coefficient at both sides of the

cooling tower are the most sensitive parameter to changes of the equivalent surface roughness. The computed value of maximum negative coefficient of pressure for seven cases with various surface roughnesses are compared with the VGB guidelines in Table 5. The values of maximum negative coefficient computed in present work are compared with experimental measurement reported from the previous researchers [1] and VGB guideline in the following figure (Fig. 16). As can be seen, the numerical results follow the nonlinear inverse relation between the height/spacing ratios (h/a) and the maximum negative (minimum) pressure coefficient. The VGB guideline proposes a piecewise constant values of maximum negative pressure coefficient ($C_p = -1$), but that is not the case for experimental measurement and numerical results. This makes major differences particularly for large value of height/spacing ratios ($0.025 < h/a < 0.1$).

The result of VGB code prediction and numerical model for the case of smooth wall are compared in Fig. 17 to show the differences in more detail. As can be seen, there are some differences, the computed results present trend similar to VGB suggestions. Positive coefficient of pressure computing at upstream stagnation point ($\theta = 0$) is identical. But the constant value of negative pressure computing at downstream part of the cooling tower ($110 < \theta < 180$) is around half of VGB prediction. Moreover, despite of relative equality of maximum negative pressure in both side of cooling tower, the maximum pressure occurs with some delay. The changing of the position of maximum pressure could affect the total wind force in the direction of wind flow. It seems these differences relates to the hyperbolic shape of cooling tower, because the coefficient of pressure for cylindrical tower is used for other tower shapes by VGB. However 3D nature of fluid flow around

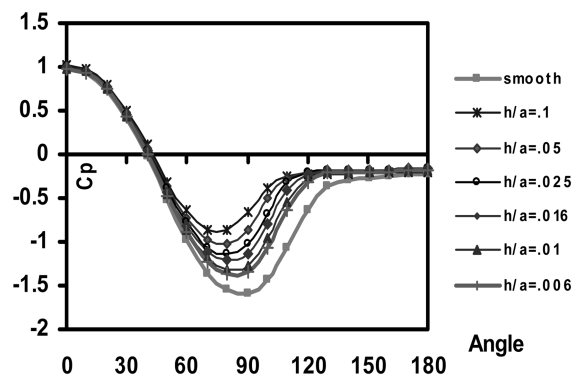


Fig. 15 Circumferential distribution of the coefficient of pressure at throat level of a full scale cooling tower for various values of h/a

Table 5 Comparison between computed maximum negative pressure and VGB guidelines

Case	h/a	VGB code	Computed
No.1	0.1	-1	-0.85
No.2	0.05	-1	-1.015
No.3	0.025	-1.1	-1.14
No.4	0.016	-1.2	-1.21
No.5	0.01	-1.3	-1.3
No.6	0.006	-1.4	-1.36
No.7	smooth	-1.6	-1.58

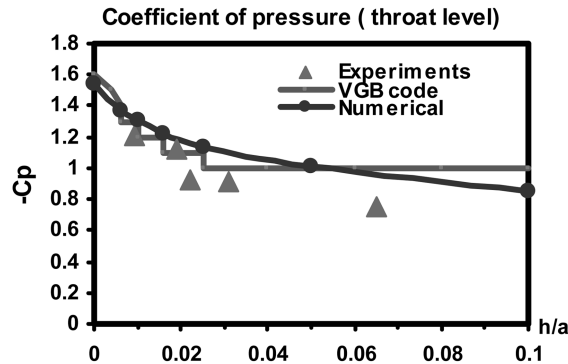


Fig. 16 Circumferential distribution of the minimum coefficient of pressure at throat level

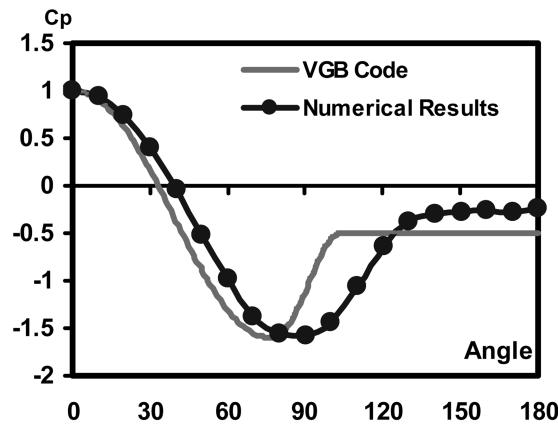


Fig. 17 Comparison the numerical result and VGB prediction of circumferential distribution of the pressure coefficient at throat level of the cooling tower for smooth surface

hyperbolic cooling towers may affect the distribution, position and the value of negative pressure especially for throat level with maximum vertical curvature.

8. Conclusions

In this paper, the concept of sand grain roughness is utilized for considering the wind ribs effects on turbulent flow field. In order to consider the effect of height and spacing of the external wind, a relation for determination of equivalent surface roughness introduced as $K_s = C(h/a)h$ (with $C = 20E/C_s$). The introduced technique for modeling equivalent roughness of cooling tower's external ribs in conjunction with the proper turbulent model provides an efficient and accurate means for computing the distribution of wind pressure on external surface of cooling tower shell. Using a FLOTTRAN module of ANSYS FE package (CFD analyzer), the results of the proposed modeling strategy are compared with the wind pressure distribution suggested by VGB (German guideline for cooling tower design) for a full scale cooling tower. From the numerical experiments for various height/spacing ratios of external wind ribs and following remarks are concluded. The maximum positive and negative pressure values at upstream face of the cooling tower follow the VGB guide-line. However, the computed negative pressures at downstream face of the cooling

tower, particularly for the cases with large height/spacing ratios, are slightly less than those suggested by VGB. The position of maximum computed negative pressure values on both sides of the cooling tower shell are different from the corresponding values suggested by VGB guideline. VGB guideline proposes a constant value for the negative pressure for large values of ribs height/spacing ($0.025 < h/a < 0.1$), while, the computational results present a continuous reduction trend on the maximum negative pressure by increasing the ribs height/spacing (h/a).

Acknowledgement

The support of BOLAND-PAYEH Company for completing this research work is greatly acknowledged.

References

- Cebeci, T. and Bradshaw, P. (1977), *Momentum Transfer in Boundary Layers*, Hemisphere Publishing Corporation, New York.
- Fisenko, S.P. and Petrushik, A.I. (2005), "Towards to the control system of mechanical draft cooling tower of film type", *Int. J. Heat Mass Transfer*, **48**, pp. 31-35.
- Fisenko, S.P., Brin, A.A. and Petrushik, A.I. (2004), "Evaporative cooling of water in a mechanical draft cooling tower", *Int. J. Heat Mass Transfer*, **47**, pp. 167-177.
- Fisenko, S.P., Petrushik, A.I. and Solodukhin, A.D. (2002), "Evaporative cooling of water in a natural draft cooling tower", *Int. J. Heat Mass Transfer*, **45**, pp. 4683-4694.
- Launder, B.E. and Spalding, D.B. (1974), "The numerical computation of turbulent flows", *Comput Methods Appl. Mech Eng.*, **3**, pp. 269-289.
- Liu, R.-F., Shen, G.-H. and Sun, B.-N. (2006), "Numerical simulation study of wind load on large hyperbolic cooling tower", *Gongcheng Lixue/Engineering Mechanics*, **23**, Issue SUPPL., June, Pages 177-183 (in Chinese)
- Niemann, H.J. (1980), "Wind effects on cooling-tower shells", *J. Struct. Eng., ASCE*, **106**(3), pp. 643-61.
- Niemann, H.J. and Kopper H. D. (1998), "Influence of adjacent buildings on wind effects on cooling towers", *Eng. Struct.*, **20**(10), pp. 874-80.
- Niemann, H.J. and Ruhwedel, J. (1980), "Full-scale and model tests on wind induced, static and dynamic stresses in cooling tower shells", *Eng. Struct.*, **2**, 81-89.
- Orlando, M. (2001), "Wind-induced interference effects on two adjacent cooling towers", *Eng. Struct.*, **23**(8), pp. 979-992.
- Sabbagh-Yazdi, S.R., Torbati, M. Azad, F.M. and Haghghi, B. (2007), "Computer simulation of changes in the wind pressure due to cooling towers-buildings interference", *WSEAS Transactions on Mathematics*, **6**(1), pp. 205-214.
- Schlichting, H. (1968), *Boundary-layer Theory*, Mc Graw-Hill, 6th edition.
- Sun, Tien-Fun and Zhou, Liang Mao (1983), "Wind pressure distribution around a rib less hyperbolic cooling tower", *J. Wind Eng. Ind. Aerodyn.; Issue 1-3*, Pages. 181-192.
- VGB Guideline (2005), "*Structural Design of Cooling Towers*", VGB-Technical Committee, "Civil engineering problems of cooling towers", Essen, Germany.
- White, F.M. (1991), *Viscous Fluid Flow*, Mc Graw-Hill, Second edition
- Zhai, S. and Fu, Z. (2001), "Numerical investigation of the adverse effect of wind on the heat transfer performance of two natural draft cooling towers in tandem arrangement", *Acta Mechanica Sinica*, **17**(1), 24-34.
- Zhai, Z. and Fu, S. (2002), "Modeling the airflow around cooling towers with multi-block CFD", *In The 4th International ASME/JSME/KSME Symposium, Canada.*
- Zhai, Z. and Fu, S. (2006), "Improving cooling efficiency of dry-cooling towers under cross-wind conditions by using wind-break methods", *Applied Thermal Engineering*, **26**, 1008-1017.